physica status solidi b
www.pss-b.com

Mean Square Relative Displacements in a Flat Graphene Monolayer

Clóves Gonçalves Rodrigues, Wesley Pacheco Calixto, and José Nicodemos Teixeira Rabelo*

The mean square relative atomic displacements (MSRD) in a flat graphene monolayer are investigated in the approximation of weak anharmonicity. Numerical results, for not very high temperatures, are calculated using a parametric interatomic potential constructed specifically for graphene. In summary, our results show an overall increase in the MSRD as the interatomic distances increase, the MSRD in the direction of the straight line connecting two pairs of atoms are smaller than perpendicular ones, and in comparison with other two-dimensional lattices, the MSRD in graphene lattice are greater than those in the hexagonal and square lattices.

1. Introduction

Mean square relative atomic displacements (MSRD) represent a key parameter in characterizing lattice dynamics. They express the effective amplitudes of atomic lattice vibrations in crystals[1,2] and are a straightforward and useful tool for comparisons with experimental data.[3] In this work, we derive analytical expressions for MSRD and investigate them numerically in an important range of temperatures. For this, we apply the correlative method of unsymmetrized self-consistent field (CUSF)[4–9], which is an efficient theory that has been developed to describe anharmonicity in solids.

C. G. Rodrigues
Escola Politécnica e de Artes
Pontifícia Universidade Católica de Goiás
CP 86, 74605-010 Goiania, Goias, Brazil
E-mail: cloves@pucgoias.edu.br

W. P. Calixto
Technology Research and Development Center
Federal Institute of Goias
Goiania 74055-110, Goias, Brazil

J. N. Teixeira Rabelo
Instituto de Física
Universidade Federal de Goiás
74001-970 Goiania, Goias, Brazil

The ORCID identification number(s) for the author(s) of this article can be found under https://doi.org/10.1002/pssb.202500255.

DOI: 10.1002/pssb.202500255

The CUSF method yields accurate results for the thermodynamic properties of strongly anharmonic crystals with a variety of lattice structures and bonding types. It has been successfully applied to van der Waals crystals,[10,11] ionic crystals,[12] fullerites,[13,14] and even to sodium[15,16] using an effective interionic potential.[17,18] The CUSF approach is suitable not only for ideal anharmonic crystals but also for systems containing lattice defects and surfaces.[19–25] This versatility enables the investigation of structural, dynamical, and thermodynamic properties, with results showing good agreement with available experimental data up to melting temperatures.[26]

The statistical perturbation theory employed in the CUSF method enhances the accuracy of anharmonic contributions to the thermodynamic functions of crystals by accounting for dynamical interatomic correlations at intermediate and long distances. This approach enables the calculation of MSRD in anharmonic crystals, including those with strong anharmonicity.

Based on the CUSF approach,[4–9] general formulas were derived for the MSRD in crystals, incorporating anharmonic terms up to fourth order.[27–29] These expressions have been applied to calculate these displacements in 1D linear chains,[28,30] as well as in 2D[29,31,32] and 3D crystal models.[13,33–37]

In the present study, the CUSF method is employed to calculate the mean square relative atomic displacements (MSRD) in a flat graphene monolayer under the weak anharmonicity approximation, which is valid at moderately low temperatures. For the numerical calculations, we adopt the parametric interatomic potential proposed specifically for graphene by Tewary and Yang.[38–40]

2. General Relations

In the zeroth-order approximation of the CUSF method, the total potential energy of the crystal, U, is replaced by a sum of individual self-consistent potentials, u_i, each corresponding to an atom undergoing anharmonic vibrations around its equilibrium lattice position,

$$U^0(\boldsymbol{r}_1, \boldsymbol{r}_2, \ldots, \boldsymbol{r}_N) = \sum_{i=1}^{N} u_i(\boldsymbol{r}_i) \tag{1}$$

in this context, the phase probability distribution is approximated as a product of single-particle probability densities, whose configurational components are denoted by

$$w_i(\boldsymbol{r}_i) = \frac{e^{-u_i(\boldsymbol{r}_i)/\Theta}}{\int e^{-u_i(\boldsymbol{r}_i)/\Theta} d\boldsymbol{r}_i} \tag{2}$$

both $w_i(\boldsymbol{r}_i)$ and the self-consistent potentials $u_i(\boldsymbol{r}_i)$ are determined by the fundamental equations of the CUSF method.[5–8] In Equation (2), $\Theta = k_B T$ is the absolute temperature in energy units (here, k_B represents the Boltzmann constant). Subsequently, the phase probability density in the configurational space is expressed as

$$w^{(N)}(\boldsymbol{r}_1, \boldsymbol{r}_2, \ldots, \boldsymbol{r}_N) = A e^{-U'/\Theta} \prod_{i=1}^{N} w_i(\boldsymbol{r}_i) \tag{3}$$

where

$$A^{-1} = \int e^{-U'/\Theta} \prod_{i=1}^{N} w_i(\boldsymbol{r}_i) d\boldsymbol{r}_i \tag{4}$$

and

$$U'(\boldsymbol{r}_1, \boldsymbol{r}_2, \ldots, \boldsymbol{r}_N) = U - U^0 \tag{5}$$

is treated as a perturbation. Consequently, when calculating statistical averages of functions dependent on atomic coordinates, expansions of Equation (3) and (4) can be performed as power series in the small parameter U'/Θ.

In CUSF method,[4–8] the mean square relative atomic displacements for two atoms i and j in a crystal with displacements $q_i = \boldsymbol{r}_i - \hat{A}n_i$, are written as

$$D_{aa}(ij) = \overline{(q_{ia} - q_{ja})^2} = \overline{(q_{ia})^2} + \overline{(q_{ja})^2} - 2\overline{q_{ia}q_{ja}} \tag{6}$$

where $\overline{(q_{ia})^2}$ are the variances of the atomic positions, $\overline{q_{ia}q_{ja}}$ are the interatomic correlation moments between atoms i and j in a crystal, $\hat{A}$ is the lattice matrix, n_i are vectors with integer components, and a denotes the Cartesian components of atomic displacements (being $a = x, y$ in a 2D lattice). For a perfect crystal $\overline{(q_{ia})^2} = \overline{(q_{ja})^2}$.

We shall consider here the case of central pairwise interatomic forces

$$U(\boldsymbol{r}_1, \boldsymbol{r}_2, \ldots, \boldsymbol{r}_N) = \frac{1}{2}\sum_{i \neq j} \Phi(|\boldsymbol{r}_i - \boldsymbol{r}_j|) \tag{7}$$

By expanding Equation (1) and (7) in a power series of atomic relative displacements and retaining anharmonic terms up to fourth order,[6,7] the perturbation potential given in Equation (5) can be written in the form

$$U' = U'_2 + U'_3 + U'_4 \tag{8}$$

where

$$U'_2 = -\frac{1}{2}\sum_{i \neq j}\sum_{\alpha,\beta} \Phi_{ij}^{\alpha\beta} q_{i\alpha} q_{j\beta} \tag{9}$$

$$U'_3 = -\frac{1}{2}\sum_{i \neq j}\sum_{\alpha,\beta,\gamma} \Phi_{ij}^{\alpha\beta\gamma} q_{i\alpha} q_{i\beta} q_{j\gamma} \tag{10}$$

$$U'_4 = -\sum_{i \neq j}\sum_{\alpha,\beta,\gamma} \Phi_{ij}^{\alpha\beta\gamma\delta} \left[\frac{q_{i\alpha}q_{i\beta}q_{i\gamma}q_{j\delta}}{6} - \frac{q_{i\alpha}q_{i\beta}(q_{j\gamma}q_{j\delta} - \overline{q_{j\gamma}q_{j\delta}}^0)}{8} - \frac{\overline{q_{i\alpha}q_{i\beta}}^0 \overline{q_{j\gamma}q_{j\delta}}^0}{8}\right] \tag{11}$$

The Greek letters α, β, γ, and δ stand for Cartesian components, and the zero attached to the bar denotes averaging over the unperturbed distribution, that is, over (3) when $U' = 0$ and $A = 1$. In Equations (9)–(11), the following notation is used for the derivatives of the interatomic potential

$$\Phi_{ij}^{\alpha\beta\ldots} = \left[\frac{\partial \cdots \Phi(|\boldsymbol{r}|)}{\partial x_\alpha \partial x_\beta \ldots}\right]_{\boldsymbol{r}=\hat{A}(n_i - n_j)} \tag{12}$$

In Equation (12), all Greek indices are free.

In this case, by using Equations (8)–(11) and including anharmonic terms up to fourth order, we obtain the following expression for the variances of the atomic positions[28]

$$\begin{aligned}
\overline{(q_{ia})^2} = {} & \overline{a_i^2}^0 + \frac{1}{2\Theta^2}\sum_k \Phi_{\alpha\beta}(ik)\Phi_{\gamma\delta}(ik) \\
& \times \left[\overline{\beta_k\delta_k}^0 \overline{a_i^2\alpha_i\gamma_i}^0 + \overline{a_i^2}^0 \overline{\alpha_i\gamma_i}^0\right] \\
& + \frac{1}{8\Theta^2}\sum_k \Phi_{\alpha\beta\gamma}(ik)\Phi_{\delta\varepsilon\xi}(ik) \\
& \times \left[\overline{\gamma_k\xi_k}^0 \left(\overline{a_i^2\alpha_i\beta_i\delta_i\varepsilon_i}^0 - \overline{a_i^2}^0 \overline{\alpha_i\beta_i\delta_i\varepsilon_i}^0\right)\right. \\
& - 2\overline{\delta_i\varepsilon_i}^0 \overline{\gamma_k\xi_k}^0 \left(\overline{a_i^2\alpha_i\beta_i}^0 - \overline{a_i^2}^0 \overline{\alpha_i\beta_i}^0\right) \\
& \left. + \left(\overline{a_i^2\alpha_i\delta_i}^0 - \overline{a_i^2}^0 \overline{\alpha_i\delta_i}^0\right)\left(\overline{\beta_k\gamma_k\varepsilon_k\xi_k}^0 - \overline{\beta_k\gamma_k}^0 \overline{\varepsilon_k\xi_k}^0\right)\right] \\
& + \frac{1}{6\Theta^2}\sum_k \Phi_{\alpha\beta}(ik)\Phi_{\gamma\delta\varepsilon\xi}(ik) \\
& \times \left[\overline{\beta_k\xi_k}^0 \left(\overline{a_i^2\alpha_i\gamma_i\delta_i\varepsilon_i}^0 - \overline{a_i^2}^0 \overline{\alpha_i\gamma_i\delta_i\varepsilon_i}^0\right)\right. \\
& \left. + \overline{\beta_k\delta_k\varepsilon_k\xi_k}^0 \left(\overline{a_i^2\alpha_i\gamma_i}^0 - \overline{a_i^2}^0 \overline{\alpha_i\gamma_i}^0\right)\right]
\end{aligned} \tag{13}$$

and for the interatomic correlation moments[28]

$$\begin{aligned}\overline{q_{ia}q_{ja}} = {} & \frac{1}{\Theta}\Phi_{\alpha\beta}(ij)\overline{a_i\alpha_i}^0\overline{b_j\beta_j}^0 + \frac{1}{6\Theta}\Phi_{\alpha\beta\gamma\delta}(ij) \\ & \times \left(\overline{a_i\alpha_i\gamma_i\delta_i}^0\overline{b_j\beta_j}^0 + \overline{a_i\alpha_i}^0\overline{b_j\beta_j\gamma_j\delta_j}^0\right) \\ & + \frac{1}{\Theta^2}\sum_k \Phi_{\alpha\gamma}(ik)\Phi_{\beta\delta}(jk)\overline{a_i\alpha_i}^0\overline{b_j\beta_j}^0\overline{\gamma_k\delta_k}^0 \\ & - \frac{1}{4\Theta^2}\Phi_{\alpha\beta\gamma}(ij)\Phi_{\delta\varepsilon\xi}(ij)\overline{a_i\alpha_i\gamma_i\delta_i}^0\overline{b_j\beta_j\varepsilon_j\xi_j}^0 \\ & + \frac{1}{4\Theta^2}\sum_k \Phi_{\alpha\beta\gamma}(ik)\Phi_{\delta\varepsilon\xi}(jk)\overline{a_i\alpha_i}^0\overline{b_j\delta_j}^0\overline{\gamma_k\delta_k}^0 \\ & \times \left(\overline{\beta_k\gamma_k\varepsilon_k\xi_k}^0 - \overline{\beta_k\gamma_k}^0\overline{\varepsilon_k\xi_k}^0\right) + \frac{1}{4\Theta^2}\Phi_{\alpha\beta\gamma}(ij) \\ & \times \sum_k \Phi_{\delta\varepsilon\xi}(jk)\left(\overline{a_i\alpha_i}^0\overline{b_j\beta_j\gamma_j\delta_j}^0\right. \\ & \left. - \Phi_{\delta\varepsilon\xi}(ik)\overline{b_j\beta_j}^0\overline{a_i\alpha_i\gamma_i\delta_i}^0\right)\overline{\varepsilon_k\xi_k}^0 \\ & - \frac{1}{4\Theta^2}\Phi_{\alpha\beta}(ij)\Phi_{\gamma\delta\varepsilon\xi}(ij)\overline{a_i\alpha_i\gamma_i\delta_i}^0\overline{b_j\beta_j\varepsilon_j\xi_j}^0 \\ & + \frac{1}{6\Theta^2}\sum_k \left[\Phi_{\alpha\gamma}(ik)\Phi_{\beta\delta\varepsilon\xi}(jk) + \Phi_{\beta\gamma}(jk)\Phi_{\alpha\delta\varepsilon\xi}(ik)\right] \\ & \times \overline{a_i\alpha_i}^0\overline{b_j\beta_j}^0\overline{\gamma_k\delta_k\varepsilon_k\xi_k}^0 \\ & + \frac{1}{6\Theta^2}\sum_k \left[\Phi_{\alpha\gamma}(ik)\Phi_{\beta\delta\varepsilon\xi}(jk)\overline{a_i\alpha_i}^0\overline{b_j\beta_j\delta_j\varepsilon_j}^0\right. \\ & \left. + \Phi_{\beta\gamma}(jk)\Phi_{\alpha\delta\varepsilon\xi}(ik)\overline{b_j\beta_j}^0\overline{a_i\alpha_i\delta_i\varepsilon_i}^0\right]\overline{\gamma_k\xi_k}^0 \end{aligned} \tag{14}$$

In Equations (12)–(14), the Latin indices a and b are fixed, whereas the Greek indices α, β, γ, δ, ε, and ξ are free. To abbreviate the notation, in the right-hand side of Equation (13) and (14), q_{a_i}, q_{α_i},..., are written as a_i, α_i,..., and the moments in the zeroth-order approximation of the CUSF method $\overline{q_{i\alpha}q_{i\alpha}\ldots}^0$ are written as $\overline{a_i\alpha_i\ldots}^0$. In Equation (13) and (14), the summation extends over all k except for $k = j$, and in the case of short-range forces, one can restrict the summation over the nearest neighbors of the atoms i and j. In Equation (13) and (14), only moments of type $\overline{q_\alpha^2}^0$, $\overline{q_\alpha^2 q_\beta^2}^0$, and $\overline{q_\alpha^2 q_\beta^4}^0$ are nonzero. The moments on the right-hand side of Equation (13) and (14) are calculated by the expression

$$\overline{q_\alpha q_\beta \ldots}^0 = \int \boldsymbol{q}_\alpha \boldsymbol{q}_\beta \ldots w^0(\boldsymbol{q})d\boldsymbol{q} \tag{15}$$

which can be expressed in terms of Θ and the derivatives of the interatomic potential (see Equation (12)). If interatomic forces are sufficiently short ranged, then we can retain only derivatives of nearest-neighbor potentials.

3. Graphene Monolayer

Graphene is one of the allotropic forms of carbon, as well as diamond, graphite, carbon nanotubes, and fullerenes.[41,42] This material can be considered as revolutionary as plastic and silicon. When produced with high quality, it can be very resistant, light, almost transparent, and an excellent conductor of heat and electricity.[43] Consisting of a flat sheet of densely packed carbon atoms in a 2D honeycomb lattice, it is an ingredient for graphitic materials of other dimensions, such as fullerenes, multilayer graphene, and nanotubes. Graphene has great potential for various technological and industrial applications such as medicine, agriculture, construction, communication, nanotechnology, military, etc.[44,45] **Figure 1** shows the simplest model, a fragment of a graphene, a honeycomb lattice.

For any given pair of atoms, we adopt a coordinate system in which the x-axis is aligned with the line connecting the corresponding lattice points. The MSRD are calculated for the nearest and third neighbors using the coordinate system $x \times y$, and for second neighbors, the system $x' \times y'$ (see Figure 1). For the second neighbors, the following expressions are used: $x' = x\cos(\phi) + y\sin(\phi)$ and $y' = y\cos(\phi) - x\sin(\phi)$, with $\phi = \pi/6$, that is a rotation of $\pi/6$ around the crystallographic z-axis.

The notation D_{xx} is used to stand for the MSRD in the direction of the straight line connecting corresponding atoms i and j, and the notation D_{yy} for the MSRD perpendicular to the line connecting the atoms i and j (see Figure 1). Consequently, considering only nearest-neighbor interactions and weakly anharmonic approximation, we obtain for the graphene monolayer the expressions

$$D_{xx}(1) = \frac{4\Theta}{3f}\left[1 + \frac{\Theta}{9f^2}\left(\frac{2h}{3} + \frac{5g^2}{3f} - \frac{4g}{3r_0} + \frac{25f}{r_0^2}\right)\right] \tag{16}$$

$$D_{xx}(2) = \frac{2\Theta}{f}\left[1 + \frac{\Theta}{27f^2}\left(-28h + \frac{31g^2}{f} + \frac{14g}{r_0} + \frac{457f}{3r_0^2}\right)\right] \tag{17}$$

$$D_{yy}(1) = \frac{20\Theta}{9f}\left[1 + \frac{\Theta}{5f^2}\left(-\frac{8h}{3} + \frac{3g^2}{f} + \frac{20g}{9r_0} + \frac{13f}{r_0^2}\right)\right] \tag{18}$$

$$D_{yy}(2) = \frac{62\Theta}{27f}\left[1 + \frac{\Theta}{3f^2}\left(-\frac{50h}{31} + \frac{113g^2}{62f} + \frac{25g}{31r_0} + \frac{493f}{62r_0^2}\right)\right] \tag{19}$$

$$D_{xx}(k) = D_{yy}(k) = \frac{20\Theta}{9f}\left[1 + \frac{\Theta}{15f^2}\left(-8h + \frac{9g^2}{f} + \frac{2g}{r_0} + \frac{41f}{r_0^2}\right)\right] \tag{20}$$

with $k \geq 3$.

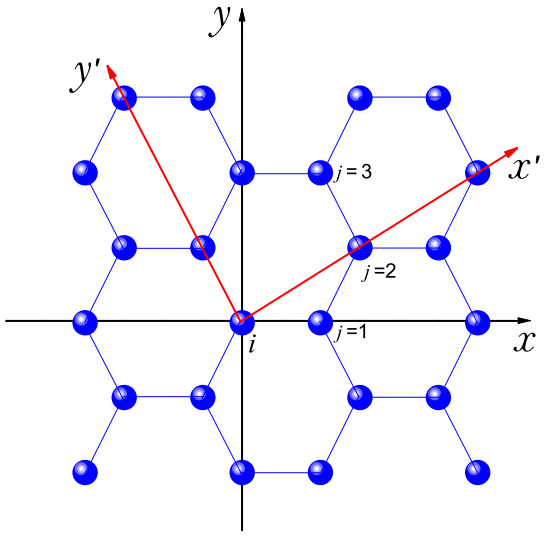

Figure 1. Fragment of a graphene lattice.

In Equations (16)–(20), r_0 is the minimum point of the interatomic potential and $e = \Phi^{(I)}(r_0)$, $f = \Phi^{(II)}(r_0)$, $g = \Phi^{(III)}(r_0)$, and $h = \Phi^{(IV)}(r_0)$ are the second, third, and fourth derivatives of the potential $\Phi(r)$ in the point r_0 (see Equation (13)).

4. Results

To obtain numerical estimates, we employ the parametric interatomic potential for graphene developed by Tewary and Yang.[38] The authors have later used this potential to investigate the MSRD at zero temperature.[39] Despite its simplicity, this interatomic potential provides good results on the thermodynamic properties of a graphene monolayer (see, for example, references[46–48]). It has the form

$$\Phi(r) = \frac{\varepsilon}{B - A}\left[\frac{B}{e^{A(r-r_0)}} - \frac{A}{e^{B(r-r_0)}}\right] \tag{21}$$

where $\varepsilon = 4.93$ eV,[40] $A = 2.69$ Å^{-1}, [38] $B = 3.28$ Å^{-1},[38] $r_0 = 1.42$ Å,[40] being ε the depth of the potential well. The values of the derivatives of the Tewary-Yang interatomic potential present in Equation (16)–(20) are: $e = 0$, $f = 13.37\varepsilon/r_0^2$, $g = -98.21\varepsilon/r_0^3$, and $h = 543.02\varepsilon/r_0^4$.

Figure 2 and **3** show, respectively, the components $D_{xx}(n)$ and $D_{yy}(n)$ of the MSRD between the first (black dot line), second (red dash line), and third (blue solid line) neighbors in a graphene monolayer. In general, the MSRD increase as the interatomic distance increases.

Figure 4 shows a comparison between the components $D_{xx}(2)$ and $D_{yy}(2)$ of the MSRD for second neighbors in a graphene monolayer. It is possible to notice that the difference between the two curves increases with increasing temperature. A similar behavior also occurs for first neighbors: $D_{xx}(1)$ and $D_{yy}(1)$. Additionally, **Figure 5** shows MSRD for first, second, and third neighbors in a graphene monolayer for a fixed temperature ($\Theta/\varepsilon = 0.20$). One can notice that the MSRD in the direction of the straight line connecting two pairs of atoms are smaller than the perpendicular ones, and that the MSRD increase as

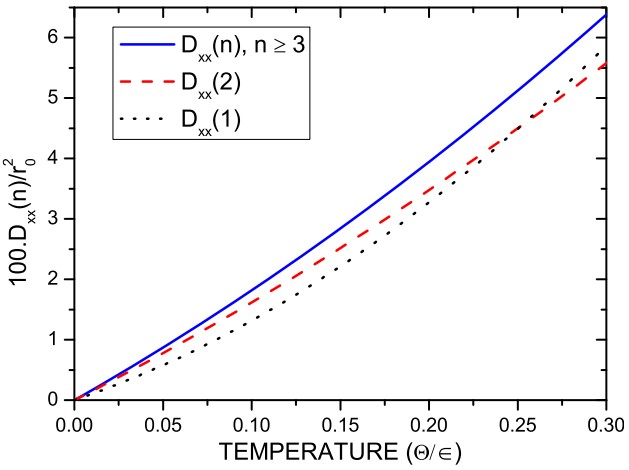

Figure 2. MSRD in the direction of the straight line connecting atoms i and j in graphene.

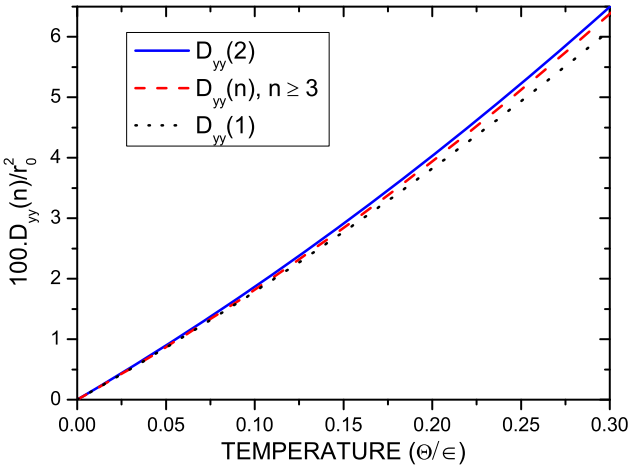

Figure 3. MSRD perpendicular to the direction of the straight line connecting atoms i and j in graphene.

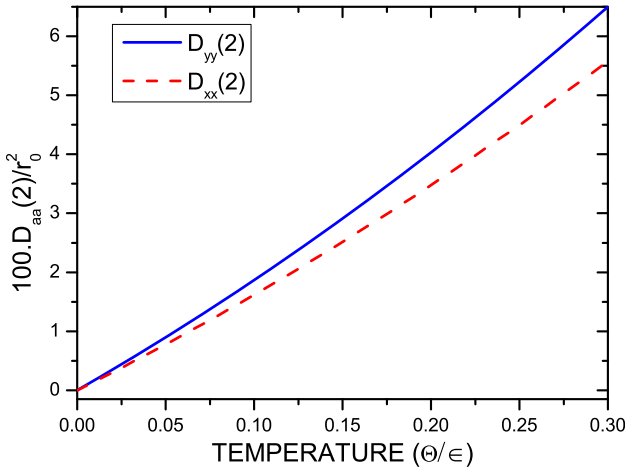

Figure 4. MSRD for second neighbors: $D_{yy}(2)$ (blue solid line) and $D_{xx}(2)$ (red dash line).

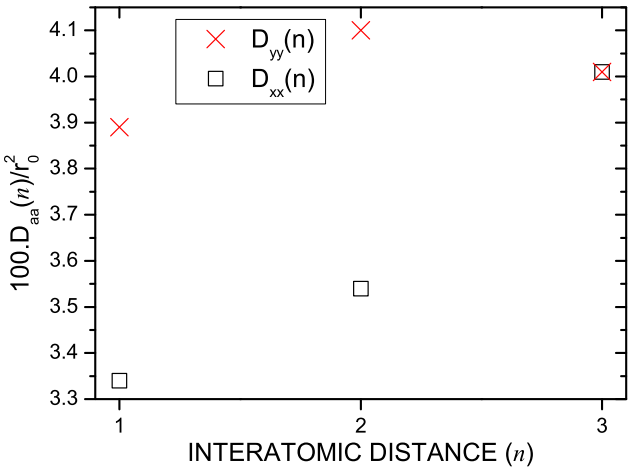

Figure 5. MSRD as a function of n for a fixed temperature ($\Theta/\varepsilon = 0.20$).

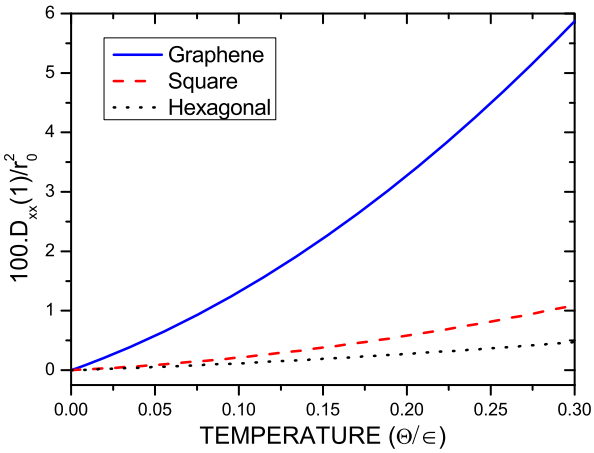

Figure 6. MSRD in the direction of the straight line connecting the nearest neighbors in: hexagonal (black dot line), square (red dash line), and graphene (blue solid line) lattices.

the interatomic distance increases. As demonstrated in the previous section $D_{xx}(3) = D_{yy}(3)$ (see Equation (20)).

Figure 6 shows the MSRD in the direction of the straight line connecting the nearest neighbors, $D_{xx}(1)$, in hexagonal (black dot line), square (red dash line), and graphene (blue solid line) lattices. For the calculation of the MSRD in hexagonal[31] and square[32] lattices, the Lennard-Jones potential was employed. It can be seen that the greater the coordination number, Z, the less the MSRD: graphene lattice ($Z = 3$), square lattice ($Z = 4$), and hexagonal lattice ($Z = 6$).

5. Final Comments

In this article, we employed the correlative method of the CUSF to calculate the MSRD in a flat graphene monolayer, within the approximation of weak anharmonicity. A parametrized interatomic potential specifically developed for graphene (proposed by Tewary and Yang) was used to obtain the numerical estimates.

The focus on MSRD in a flat graphene monolayer, especially in the approximation of weak anharmonicity, is a relevant topic, particularly for understanding the mechanical and thermal properties of graphene at the atomic level. The study's aim to explore MSRD and its dependence on temperature and interatomic distances is valuable. Such insights are critical for developing theoretical models and designing graphene-based materials.

Summarizing the results: a) In general, the MSRD increase as the interatomic distance increases; b) The MSRD in the direction of the straight line connecting two pairs of atoms are smaller than perpendicular ones; c) In comparison with other 2D lattices, the MSRD in graphene lattice are greater than those in the hexagonal[31] and square[32] lattices.

The present study has some limitations. Previous work has shown that the MSRD in graphene is not only temperature dependent but also depends on the size of the system,[49] and also closely related to the thermal expansion of graphene.[50] Furthermore, we once again note that the anharmonicity of lattice vibrations in 2D crystals is expected to be strong.[51–55] Therefore, a logical continuation of this study would be to move toward a strong anharmonicity approximation. The influence of strong anharmonicity on the dynamic properties of graphene monolayer will be addressed in a future paper.

Acknowledgements

The Article Processing Charge for the publication of this research was funded by the Coordenação de Aperfeiçoamento de Pessoal de Nível Superior - Brasil (CAPES) (ROR identifier: 00x0ma614).

Conflict of Interest

The authors declare no conflict of interest.

Author Contributions

Clóves Gonçalves Rodrigues: conceptualization (equal); data curation (equal); formal analysis (equal); investigation (equal); methodology (equal); project administration (equal); software (equal); supervision (equal); validation (equal); visualization (equal); writing—original draft (equal); writing—review & editing (equal). **Wesley Pacheco Calixto**: data curation (equal); formal analysis (equal); investigation (equal); methodology (equal); validation (equal); visualization (equal); writing—review & editing (equal). **Jose Nicodemos Teixeira Rabelo**: data curation (equal); formal analysis (equal); investigation (equal); methodology (equal); validation (equal); visualization (equal); writing—review & editing (equal).

Data Availability Statement

The data that support the findings of this study are available from the corresponding author upon reasonable request.

Keywords

anharmonic crystals, graphene, lattice dynamics

Received: May 15, 2025
Revised: July 13, 2025
Published online:

[1] G. Leibfried, *Gittertheorie Der Mechanischen and Thermischen Eingenschaften Der Kristalle*, Springer, Berlin **1955**.
[2] Y. P. Terletskii, *Statistical Physics*, North-Holland Publ. Co., Amsterdam **1971**.
[3] A. A. Maradudin, E. W. Montroll, G. H. Weiss, I. P. Ipatova, *Theory of Lattice Dynamics in the Harmonic Approximation*, Academic, New York **1971**.
[4] N. M. Plakida, T. Siklós, *Acta Phys. Hungar.* **1978**, *45*, 37.
[5] V. I. Zubov, Y. P. Terletskii, *Ann. Phys. Leipzig* **1970**, *479*, 97.
[6] V. I. Zubov, *Phys. Stat. Sol. B* **1975**, *72*, 71.
[7] V. I. Zubov, *Phys. Stat. Sol. B* **1975**, *72*, 483.
[8] V. I. Zubov, *Ann. Phys. Leipzig* **1974**, *486*, 33.
[9] V. I. Yukalov, V. I. Zubov, *Fortschr. Phys.* **1983**, *31*, 627.
[10] V. I. Zubov, *Phys. Stat. Sol. B* **1980**, *101*, 95.
[11] V. I. Zubov, N. P. Tretyakov, J. F. Sanchez, *Internat. J. Mod. Phys. B* **1995**, *9*, 3559.
[12] V. I. Zubov, S. S. Soulayman, *Kristallografiya* **1982**, *27*, 588.

[13] V. I. Zubov, C. G. Rodrigues, *Phys. Stat. Sol. B* **2000**, *222*, 471.
[14] V. I. Zubov, C. G. Rodrigues, I. V. Zubov, *Phys. Stat. Sol. B* **2003**, *238*, 110.
[15] J. F. S. Ortiz, N. P. Tretiakov, V. I. Zubov, *Phys. Stat. Sol. B* **1994**, *181*, k7.
[16] J. F. S. Ortiz, N. P. Tretiakov, V. I. Zubov, *Phys. Stat. Sol. B* **1997**, *200*, 27.
[17] N. W. Ashcroft, *Europhys. Lett.* **1991**, *16*, 355.
[18] N. W. Ashcroft, *Nature* **1993**, *365*, 387.
[19] V. I. Zubov, *Phys. Stat. Sol. B* **1982**, *111*, 417.
[20] V. I. Zubov, J. N. T. Rabelo, *Phys. Stat. Sol. B* **1986**, *138*, 433.
[21] V. I. Zubov, F. Banyeretse, N. P. Tretiakov, I. V. Mamontov, *Internat. J. Mod. Phys. B* **1990**, *4*, 317.
[22] V. I. Zubov, N. P. Tretiakov, *Phys. Stat. Sol. B* **1991**, *164*, 409.
[23] V. I. Zubov, *Int. J. Mod. Phys. B* **1992**, *6*, 367.
[24] V. I. Zubov, I. V. Mamontov, N. P. Tretiakov, *Int. J. Mod. Phys. B* **1992**, *6*, 197.
[25] V. I. Zubov, I. V. Mamontov, N. P. Tretiakov, *Int. J. Mod. Phys. B* **1992**, *6*, 221.
[26] C. G. Rodrigues, *Czech. J. Phys.* **2004**, *54*, 849.
[27] V. I. Zubov, M. F. Pascual, *Izv. Vuzov Fizika* **1984**, *27*, 67.
[28] V. I. Zubov, M. F. Pascual, J. N. T. Rabelo, *Phys. Stat. Sol. B* **1993**, *175*, 331.
[29] V. I. Zubov, M. F. Pascual, *Mod. Phys. Lett. B* **1994**, *8*, 523.
[30] V. I. Zubov, M. F. Pascual, J. N. T. Rabelo, A. C. Faria, *Phys. Stat. Sol. B* **1994**, *182*, 315.
[31] V. I. Zubov, M. F. Pascual, C. G. Rodrigues, *Modern Phys. Lett. B* **1995**, *9*, 839.
[32] M. F. Pascual, V. I. Zubov, *Modern Phys. Lett. B* **1995**, *9*, 1513.
[33] M. F. Pascual, A. L. Rosa, V. I. Zubov, *Mod. Phys. Lett. B* **1996**, *10*, 599.
[34] V. I. Zubov, M. F. Pascual, C. G. Rodrigues, *Mod. Phys. Lett. B* **1996**, *10*, 1043.
[35] C. G. Rodrigues, M. F. Pascual, V. I. Zubov, *Braz. J. Phys.* **1997**, *27*, 448.
[36] V. I. Zubov, C. G. Rodrigues, M. F. Pascual, *Int. J. Modern Phys. B* **1998**, *12*, 2869.
[37] C. G. Rodrigues, V. I. Zubov, M. F. Pascual, *Braz. J. Phys.* **1999**, *29*, 450.
[38] V. K. Tewary, B. Yang, *Phys. Rev. B* **2009**, *79*, 075442; Erratum: V. K. Tewary, B. Yang, Phys. Rev. B 2010, 81, 039904(E).
[39] V. K. Tewary, B. Yang, *Phys. Rev. B* **2009**, *79*, 125416.
[40] D. W. Brenner, O. A. Shenderova, J. A. Harrison, S. J. Stuart, B. Ni, S. B. Sinnott, *J. Phys. Condens. Matter* **2002**, *14*, 783.
[41] A. K. Geim, K. S. Novoselov, *Nat. Mater.* **2007**, *6*, 183.
[42] A. R. Urade, I. Lahiri, K. S. Suresh, *JOM* **2023**, *75*, 614.
[43] T. Lalire, C. Longuet, A. Taguet, *Carbon* **2024**, 119055.
[44] M. A. Poothanari, Y. B. Pottathara, S. Thomas, *Industrial Applications of Nanomaterials*, Elsevier, Amsterdam **2019**, pp. 205–223.
[45] S. Qamar, N. Ramzan, W. Aleem, *Synth. Met.* **2024**, *307*, 117697.
[46] Y. Magnin, G. D. Förster, F. Rabilloud, F. Calvo, A. Zappelli, C. Bichara, *J. Phys.: Condens. Matter* **2014**, *26*, 185401.
[47] J. N. T. Rabelo, L. Cândido, *J. Phys. Commun.* **2018**, *2*, 095013.
[48] J. N. T. Rabelo, *Phys. Lett. A* **2023**, *481*, 129010.
[49] K. H. Michel, S. Costamagna, F. M. Peeters, *Phys. Rev. B* **2015**, *91*, 134302.
[50] K. H. Michel, S. Costamagna, F. M. Peeters, *Phys. Status Solidi B* **2015**, *252*, 2433.
[51] A. Fasolino, J. H. Los, M. I. Katsnelson, *Nature Mater.* **2007**, *6*, 858.
[52] K. V. Zakharchenko, M. I. Katsnelson, A. Fasolino, *Phys. Rev. Lett.* **2009**, *102*, 046808.
[53] A. L. C. Silva, L. Candido, J. N. T. Rabelo, G.-Q. Hai, F. M. Peeters, *Europhys. Lett.* **2014**, *107*, 56004.
[54] P. Xu, M. Neek-Amal, S. D. Barber, J. K. Schoelz, M. L. Ackerman, P. M. Thibado, *Nat. Commun.* **2014**, *5*, 372.
[55] M. L. Ackerman, P. Kumar, M. Neek-Amal, P. M. Thibado, F. M. Peeters, S. Singh, *Phys. Rev. Lett.* **2016**, *117*, 126801.